Chapter 2. Self-Calibrated Interferometric/Intensity Based (SCIIB) Sensor Technology

The Self-Calibrated Interferometric/Intensity-Based (SCIIB) sensor technology is a novel type of fiber optic sensor technology developed by the Photonics Lab at Virginia Tech. It combines the advantages of both the interferometric-based and the intensity-based fiber optic sensors in a single system. The sensing element — sensor head is based on the Extrinsic Fabry-Perot Interferometer (EFPI) which offers high resolution and high precision with interferometric-based sensors' advantage; the signal processing technique — detection of optical signal is based on detection of optical intensity which offers simple signal processing technique with intensity-based sensors' advantage. This is called "Interferometric/Intensity-Based". The word "Self-Calibrated" indicates another benefit provided by the SCIIB technology. In traditional sensor systems, sometimes some elements inside the sensor system or some environmental factors outside the system rather than the real measurand will cause the random change of optical power in the sensor system. This will put a terrible impairment on the performance of the sensor system. For example, the optical power of the optical source will fluctuate with the change of the temperature of the optical source itself. Unintentionally bending the transmitting fiber also will make the optical power change randomly. To eliminate these errors, based on a novel technique named Split-Spectrum technique, SCIIB sensors cancel the bad effect of optical power change, which makes the system "self-calibrate" errors caused by the random optical power change. Through a proper design of the sensor, the SCIIB technology can provide absolute measurement of various parameters with the full self-compensation capability for the source power fluctuation and the fiber loss changes.

The Self-Calibrated Interferometric/Intensity-Based (SCIIB) sensor technology originates from the well-known Extrinsic Fabry-Perot Interferometer(EFPI). Thus this chapter will start with a review of fiber optic Fabry-Perot sensing techniques, then present the configuration of the SCIIB system followed by the detailed discussion of the unique signal processing method — split-spectrum technique that offers the system self-calibration capability.

2.1 Fiber Optic Fabry-Perot Interferometer Sensors

The Fabry-Perot interferometer is a very useful tool for high precision measurement, optical spectrum analysis, optical wavelength filtering, and construction of lasers [8, 9]. It is a high resolution, high throughput optical spectrometer that works on the principle of constructive interference. The Fabry-Perot interferometer is a very simple device that is based on the interference of multiple beams [10]. It consists of two partially transmitting mirrors that form a reflective cavity. Incident light enters the Fabry-Perot cavity and experiences multiple reflections between the mirrors so that the light can produce multiple interferences.

Now let's image what would happen if a light beam enters a F-P cavity between two partial reflective mirrors. The light beam is reflected back and forth between the mirrors, but at each reflection only a small fraction of the light is transmitted. The refractive index of the material is n.

The optical path length between each successive transmitted light beam is 2nd (where d is the separation of the reflecting mirrors). This leads to a phase shift between successive light beams of

$$\delta = \frac{4\pi \cdot n \cdot d}{\lambda} \qquad (2\text{-}1)$$

where λ is the light wavelength in vacuum.

If δ=N2π (N is an integer), all the transmitted lights are in phase and they will interfere constructively. If δ=Nπ (N is an integer), each pair of lights is out of phase and destructive interference will occur. If the plates are highly reflective, the intensity of the ray trapped in the cavity decreases little between reflections; the transmitted waves have almost the same amplitude and the result has almost zero intensity.

Let's consider what happens if the phase shift is Nπ. Then the first transmitted light beam will interfere destructively with the 3rd, the 2nd with the 4th etc. At this point only waves with δ=2π can be transmitted.

For mirrors with finite reflectivity, the transmitted intensity (I_t) can be given by [9]

$$\frac{I_t}{I_i} = \frac{1}{1 + \left(\frac{2r}{1-r^2}\right)^2 \sin^2\left(\frac{\delta}{2}\right)} \qquad \text{(2-2)}$$

where I_i is the incident intensity, r is the fraction of the amplitude of the wave that is reflected at each boundary. The factor $\left(\frac{2r}{1-r^2}\right)^2$ is sometimes referred to as the Finesse. The larger the Finesse, the sharper the peak around δ=2π. The result is shown in Figure 2-1.

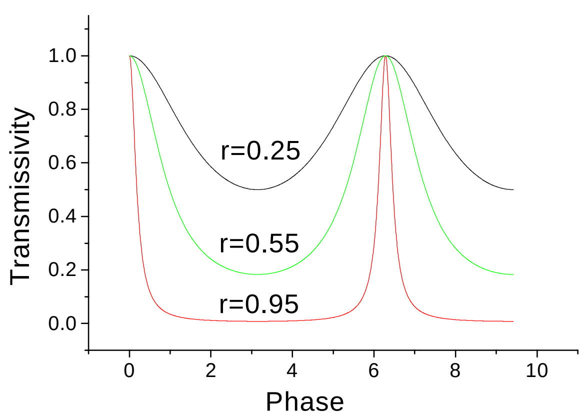

Figure 2-1. Transmissivity as a function of Phase in Fabry-Perot interferometer

According to the different behaviors of the incident light, fiber optic Fabry-Perot sensors can be classified into two types — extrinsic sensors and intrinsic sensors [11]. In extrinsic sensors, the light can be allowed to exit the fiber and be modulated in a separate zone before being relaunched into either the same or a different fiber. They form an interferometric cavity outside the fiber, and the fiber just acts as a medium to transmit light into and out of the Fabry-Perot cavity. In intrinsic sensors, the light can continue within the fiber and be modulated. They form a Fabry-Perot cavity with a section of fiber with its two endfaces cleaved or coated with reflective coatings.

2.1.1 Intrinsic Fabry-Perot Interferometer Sensor

In intrinsic sensors the fiber construction materials are deliberately chosen in order to give sensitivity to one or more parameters [11]. Often it is not cost effective to make highly specialized fibers for sensing applications; therefore intrinsic sensors may utilize readily available fiber in specialized configurations and in conjunction with sophisticated instrumentation.

Usually an Intrinsic Fabry-Perot Interferometer (IFPI) sensor is fabricated by splicing a section of special fiber with its two endfaces coated with reflective films to regular fibers. The interferometric superposition of multiple reflections at the two special fiber's endfaces generates the output signal, which is a function of the F-P cavity length, the refractive index of the special fiber, and the reflectance of the coating. The change of the F-P cavity length or the refractive index of the special fiber can be detected by tracking the interference output (either through the reflection or the transmission). Various physical or chemical parameters such as temperature, pressure and strain can be measured with a high resolution using a IFPI sensor.

2.1.2 Extrinsic Fabry-Perot Interferometer Sensor

In extrinsic sensors the performance of the device should be independent of the fiber and depend only on the nature of the sensing element, hence it offers the flexibility to design the Fabry-Perot cavity to accommodate different applications. A typical EFPI sensor configuration is shown in Figure 2-2. It consists of a cavity that is formed between an input optical fiber and a reflecting optical fiber. Although the two reflectors of forming the Fabry-Perot cavity can be the surfaces of any optical components, a very simple way to form an EFPI will be using the well-cleaved endfaces of two fibers.

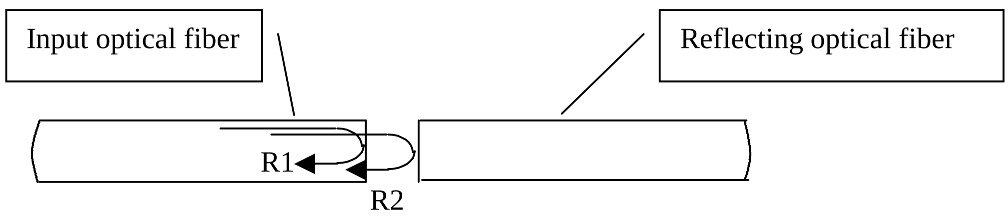

Figure 2-2. Illustration of an EFPI fiber optic sensor

As shown in Figure 2-2, the light from an optical source propagates along the input optical fiber to the Fabry-Perot cavity that is formed by the input optical fiber and the reflecting optical fiber. A fraction of this incident light R1, approximately 4%, is reflected at the endface of the input optical fiber backward the input optical fiber. The light transmitting out of the input optical fiber projects onto the fiber end face of the reflecting optical fiber. The reflected light R2 from the reflecting optical fiber is partially recoupled into the input optical fiber.

If the distance between the two end faces is less than the coherence length, Lc, of the optical source, the two reflections, R1 and R2, will produce interference fringes.

When an EFPI made of low-reflectivity mirrors is illuminated by a monochromatic light source, the response is periodic function similar to a two-beam interferometer which can be described by [11]

$$I = E_1^2 + E_2^2 + 2E_1E_2\cos\left(\frac{4\pi nd}{\lambda}\right) \qquad (2\text{-}3)$$

where E1 and E2 are the magnitudes of the electrical fields of the reflected light at two fiber ends, d is the length of the air gap of the Fabry-Perot cavity, λ is the wavelength, and n is the refractive index of the medium. When $E_1 \approx E_2$ and assuming $I_1 = E_1^2$, Equation (2-3) can be simplified as:

$$\begin{aligned} I &= 2E_1^2(1+\cos\left(\frac{4\pi nd}{\lambda}\right)) \\ &= 2I_1(1+\cos\left(\frac{4\pi nd}{\lambda}\right)) \end{aligned} \qquad (2\text{-}4)$$

According to the Equation (2-4), the interference signal from an EFPI is a function of the cavity length and refractive index of the medium inside the Fabry-Perot cavity. Via detecting the change of the interference fringes, Extrinsic Fabry-Perot interferometers can work as sensors to detect many physical parameters such as temperature [12,13], strain [14,15], pressure [16,17], vibration[18], and flow [19,20]. With advantages of such as high sensitivity, small size, simple structure, polarization independence, and great design flexibility, EFPI fiber optic sensors are attracting to be better choices in many sensing applications.

2.2. SCIIB Fiber Optic Sensor System

Figure 2-3 describes the configuration and operating principle of the SCIIB fiber optic sensor system. The system can be divided into three parts. 1) Optical section: including a broadband source, a 3-dB coupler, a sensor head, a beam-splitter and an optical filter; 2) Electronic section: including a trans-impedance amplifier for transforming the optical signal into electronic one. 3) Interface to computer: including a data acquisition system and a computer.

The light from the broadband optical source (for example an LED or SLD) is coupled into a single-mode or multimode optical fiber. Then the light propagates through a 3-dB fiber coupler to the sensor head. To eliminate the back-reflection, one branch of the coupler is index-matched with gel. The sensor head is an Extrinsic Fabry-Perot

Interferometer consisting of two optical fibers with their well-cleaved end-faces and a capillary tube so that an air-gaped low finesse Fabry-Perot cavity is formed between the two fiber endfaces, as shown in the enlarged view of the sensor head. The optical fiber and the tube are firmly bonded using a CO2 laser. Based on the EFPI principle, at first the incident light is partially reflected (~4%) at the endface of the input fiber. The transmitting light propagates across the air gap to the endface of the reflecting fiber, where a second reflection (~4%) is generated. The two reflections form the back-reflecting optical signal from the EFPI. Then the optical signal travels back along the same fiber and through the same fiber coupler to the beam-splitter, where two identical light beams — two channels with the same spectrum and intensity are produced. In one channel named Narrow Band, we use a narrow-band optical filter to extract partial spectrum of the original spectrum (for example 10 nm). The other channel named Broad Band contains the original spectrum output from the EFPI sensor head. After opto-electronic conversions via trans-impedance amplifiers, the electronic signals of the Narrow Band and the Broad Band are input into the data acquisition system for Analog-to-Digital conversions, where computer-processable digital signals are generated. Finally digital signals are processed in real time by the computer.

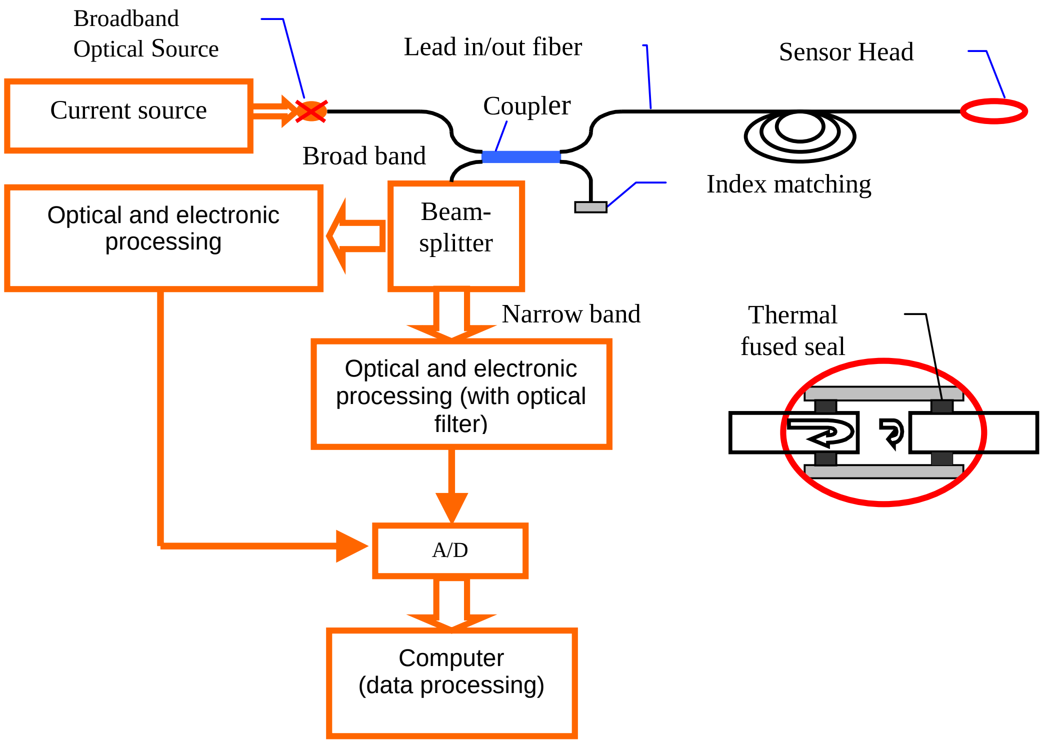

Figure 2-3. Schematic of SCIIB fiber optic sensor system

2.2.1 Split-Spectrum Technique

2.2.1.1 Coherence Length

Seen from the description of the SCIIB sensor system above, the innovation inside this system lies on the signal processing technique for dealing with the output optical signal from the 3-dB coupler. Rather than just detecting the output optical intensity with a photodetector directly like regular intensity-based sensors nor counting the interference fringe like regular interferometric-based sensors, we employ a beamsplitter to split the spectrum of output optical signal into two parts. Just as said before, one part is called Narrow Band and the other part is called Broad Band depending on whether using an optical filter or not. The light in the Broad Band remains its original spectral width of the broadband optical source (for example 80 nm) while the light in the Narrow Band has a narrower spectrum by passing it through an optical bandpass filter (for example 10 nm).

Our purpose is to get different coherence lengths of these two channels because of the principle of physical optics.

Based on the principle of physical optics, coherence of two light beams from the EFPI is dependant on relationship between their Optical Path Difference(OPD) and the coherence length of the optical source. If their OPD is greater than the coherence length of the optical source, there is effective interference between these two light beams and there is no highly visible interference fringe although they are from the same optical source. There is a phenomenon of effective interference with fringes only if their OPD is not greater than the coherence length of the optical source. So the coherence length of an optical source plays a key role in the possibility of the occurrence of the interference.

According to the principle of physical optics, the coherence length is a function of the central wavelength and the spectral width of the optical source. The coherence length Lc can be calculated by the following equation

$$L_c \approx \frac{\lambda^2}{\Delta\lambda} \qquad (2\text{-}5)$$

where λ is the central wavelength of the optical source and $\Delta\lambda$ is the spectral width of the optical source.

As described above, the two channels — the Narrow Band and the Broad Band get different spectral widths through employing an optical filter in the course of the channel of Narrow Band. The spectral width in the Narrow Band is much less than that in the Broad Band. Here, we assume that the original spectrum width of the source can be approximated as a Gaussian profile with a spectral width of $\Delta\lambda_1$, and also assume that the spectral characteristic of the optical bandpass filter is a Gaussian profile too, but with a different spectral width of $\Delta\lambda_2$. Thus the Broad Band is with a spectral width of $\Delta\lambda_1$ and the Narrow Band is with a spectral width of $\Delta\lambda_2$. With different spectral widths, these two channels thus have different coherent lengths.

2.2.1.2 Principle of Interference

Let's study the two channels' output signals in terms of optical interference. First, we define the total optical intensity I_0 of the broadband optical source (for example an LED or SLD) as

$$I_0 = \int_0^\infty i(\lambda) d\lambda \qquad (2\text{-}6)$$

where λ is the wavelength and $i(\lambda)$ is the spectral power density distribution. For convenience of calculation, we rewrite Equation (2-6) as

$$I_0 = \frac{1}{\pi}\int_0^\infty i(k) dk \qquad (2\text{-}7)$$

where the wave vector $k=2\pi/\lambda$. Because when there is only a monochromatic light beam in the interferometer, the change of the optical intensity with the change of the cavity of interferometer Δd is $2i(k)[1+\cos(2nk\Delta d)]$, so after the optical intensities of different wavelengths' light beams are overlapped together noncoherently, the result can be given by

$$I(\Delta d) = \frac{2}{\pi}\int_0^\infty i(k)[1+\cos(2nk\Delta d)]dk$$

$$= 2I_0 + \frac{2}{\pi}\int_0^\infty i(k)\cos(2nk\Delta d)dk \qquad (2\text{-}8)$$

In our case, we assume the spectral power density distribution is Gaussian profile, and we normalize the i(k) to satisfy the Equation (2-7) to obtain

$$\mathrm{i(k)} = -\frac{2\sqrt{\pi} I_0}{\Delta k} \cdot e^{-(\frac{k-k_0}{\Delta k/2})^2} \qquad (2\text{-}9)$$

where $\Delta k = -\frac{2\pi}{\lambda^2} \cdot \Delta\lambda$ and $0 \le k \le \infty$.

Hence, Equation (2-8) is transformed into the final form as the following,

$$\mathrm{I}(\Delta d) = 2I_0 + \frac{4I_0}{\sqrt{\pi}\Delta k} \cdot \int_0^{\infty} e^{-(\frac{k-k_0}{\Delta k/2})^2} \cdot \cos(2nk\Delta d)dk \qquad \text{(2-10)}$$

Equation (2-10) is the basic equation for us to calculate the output signal from the EFPI sensor as shown in the following section.

2.2.1.3 Principle of Self-Calibration

To show the principle of the SCIIB sensor, now we need to calculate the output optical intensities from the two channels. Based on the Equation (2-10), the equations for calculating the output optical intensities from the Narrow Band and the Broad Band are respectively given by,

$$\mathrm{I}_{\mathrm{narrow}}(\Delta d) = 2I_0 + \frac{4I_0}{\sqrt{\pi}\Delta k_{narrow}} \cdot \int_0^{\infty} e^{-(\frac{k-k_{0narrow}}{\Delta k_{narrow}/2})^2} \cdot \cos(2nk\Delta d)dk \qquad \text{(2-11)}$$

$$\mathrm{I}_{\mathrm{broad}}(\Delta d) = 2I_0 + \frac{4I_0}{\sqrt{\pi}\Delta k_{broad}} \cdot \int_0^{\infty} e^{-(\frac{k-k_{0broad}}{\Delta k_{broad}/2})^2} \cdot \cos(2nk\Delta d)dk \qquad \text{(2-12)}$$

where

$$\Delta k_{narrow} = -\frac{2\pi}{\lambda_{narrow}^2} \cdot \Delta\lambda_{narrow}, \qquad \Delta k_{broad} = -\frac{2\pi}{\lambda_{broad}^2} \cdot \Delta\lambda_{broad},$$

$k_{0narrow} = 2\pi/\lambda_{narrow}$, $k_{0broad} = 2\pi/\lambda_{broad}$, and I_{narrow} and I_{broad} are the output optical intensities from the Narrow Band and the Broad Band, respectively, λ_{narrow} and λ_{broad} are the central wavelengths of the Narrow Band and the Broad Band, respectively, $\Delta\lambda_{narrow}$ and $\Delta\lambda_{broad}$ are the spectral widths of the Narrow Band and Broad Band, respectively.

According to the principle of the SCIIB sensor, finally we calculate the ratio of the output optical intensity from the Narrow Band to the optical intensity from the Broad Band as the final signal result with self-calibration, which can be expressed by

$$\text{ratio} = \frac{\mathrm{I}_{\text{narrow}}(\Delta d)}{\mathrm{I}_{\text{broad}}(\Delta d)} = \frac{I_0 + \dfrac{2I_0}{\sqrt{\pi}\Delta k_{narrow}} \cdot \int_0^{\infty} e^{-(\frac{k-k_{0narrow}}{\Delta k_{narrow}/2})^2} \cdot \cos(2nk\Delta d)dk}{I_0 + \dfrac{2I_0}{\sqrt{\pi}\Delta k_{broad}} \cdot \int_0^{\infty} e^{-(\frac{k-k_{0broad}}{\Delta k_{broad}/2})^2} \cdot \cos(2nk\Delta d)dk} \tag{2-13}$$

In principle, continuously monitoring the phase change of the interference fringes just in the Narrow Band or Broad Band will already provide us with the measurement of the change of the cavity length of the sensor head. Like the output of a regular interferometer, the measurement will have ultra-high sensitivity. One period of fringe variation corresponds to an air gap change of one-half of the optical wavelength. However, due to some factors' change (for example fiber loss variations and the optical source's power drift) the optical power change in the system would introduce errors to the amplitude of the interference signal and result in a poor accuracy of the measurement. In order to reduce these adverse effects, we use the output from the Narrow Band as the signal and use Broad Band as the reference, and the SCIIB sensor's output is evaluated as the ratio of the two channels' outputs.

When fabricating a sensor head for our SCIIB sensor system, we choose the operating point of the sensor head at the point where the OPD of the Narrow Band is less than its coherent length while the OPD of the Broad Band is greater than its coherent length. Thus while the Narrow Band will get effective interference with good fringes, the Broad Band will have no effective interference. Hence, the above equation for ratio of the Narrow Band to the Broad Band can be simplified into the following form with ignoring the interference item in the Broad Band,

$$\begin{aligned}\text{ratio} &= \frac{\mathrm{I}_{\text{narrow}}(\Delta d)}{\mathrm{I}_{\text{broad}}(\Delta d)} = \frac{I_0 + \dfrac{2I_0}{\sqrt{\pi}\Delta k_{narrow}} \cdot \displaystyle\int_0^{\infty} e^{-(\frac{k-k_{0narrow}}{\Delta k_{narrow}/2})^2} \cdot \cos(2nk\Delta d)dk}{I_0} \\ &= 1 + \frac{2}{\sqrt{\pi}\Delta k_{narrow}} \cdot \int_0^{\infty} e^{-(\frac{k-k_{0narrow}}{\Delta k_{narrow}/2})^2} \cdot \cos(2nk\Delta d)dk \end{aligned} \tag{2-14}$$

From the view of the operation of the sensor system, the two channels' outputs are from the same optical source and experience the same transmission path. Thus they have almost the same behavior in terms of optical source's power fluctuation and fiber loss variations. As indicated in Equation (2-14), the ratio of the outputs from the Narrow Band to the Broad Band is only a function of the Fabry-Perot cavity length, there is no influence from the optical power I_0, thus it eliminates these two sources of errors from the final result of the measurement. This is the effect obtained from the ability of Self-Calibration of the Split-Spectrum technique.

Another important parameter of the sensor head is the fringe visibility. It is defined by

$$\nu = \frac{I_{\max} - I_{\min}}{I_{\max} + I_{\min}} \tag{2-15}$$

where I_{max} and I_{min} are the maximum and minimum intensities of the optical interference respectively. With the Gaussian profile of the spectral power density distribution of the optical source, the fringe visibility ν can be approximately estimated by [11]

$$\nu = e^{-\frac{2d}{Lc}} \tag{2-16}$$

In practice, there is a tradeoff between the good ability of Self-Calibration and good fringe visibility. On one hand, when the Fabry-Perot cavity length d formed by the input fiber end face and the reflecting fiber end face is big enough, the OPD will be large enough to get no effective interference in the Broad Band, meanwhile the optical intensity of the reflection from the reflecting fiber will be much smaller than the optical intensity of the reflection from the input fiber. At this point, the fringe visibility (described by the Fabry-Perot cavity length d in the Equation (2-16)) essentially determined by the two reflections will be worse. From the simplified Equation (2-16), we can see the bigger the cavity length d the worse the fringe visibility. However, on the other hand if we want to choose a small cavity length d for getting good visibility, the Broad Band will be not in the status of complete noncoherence, that means there still exists partial interference in the Broad Band.

To insure the proper ability of Self-Calibration of the SCIIB sensor system with good visibility, it is very important to choose an optimal initial sensor cavity length that gives us good enough fringe visibility and at the same time the interference of the reference channel is suppressed to small enough. For example, in the case for our multimode SCIIB system with an LED @ 850 nm, the initial cavity length can be chosen somewhere from 7 to 10μm.

2.2.1.4 Result of Simulations

Now we use the above equations to simulate the operation of the SCIIB sensor system. In our simulations, based on the specification of the LED @ 850 nm we use in the multimode fiber-based SCIIB sensor system, we assume I_0=1. In addition, the spectral width $\Delta\lambda$ of the LED is 80nm when the LED is operated at 50% of its maximal power allowed. So when the output power of the LED is reduced to 1/e of the peak value, the spectral width $\Delta\lambda$ (that is the spectral width of the Broad Band) is given by,

$$e^{-(\frac{0.08}{\Delta\lambda})^2} = 50\% \Rightarrow \Delta\lambda = \frac{0.08}{\sqrt{-\ln(0.5)}}\, um$$

Thus we define $\Delta\lambda_{broad}$=0.08/sqrt(-ln(0.5)) μm. Meanwhile we assume the spectral width of the bandpass filter for the Narrow Band is 10 nm, so $\Delta\lambda_{narrow}$= 10 nm.

Given the above parameters of the LED, the Lc of the Narrow Band and the Broad Band are 72.250 um and 9.03125 um, respectively according to Equation (2-5). So in practice, the initial cavity length is chosen somewhere from 7μm to 10μm according to the consideration described above. The following are the simulation results of the Narrow Band output, the Broad Band output and the ratio of the Narrow Band to the Broad Band:

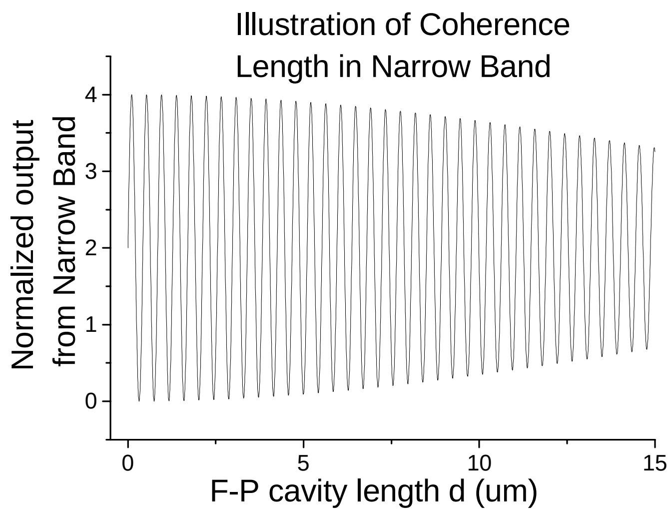

Figure 2-4. Output of Narrow Band as a function of F-P cavity length d

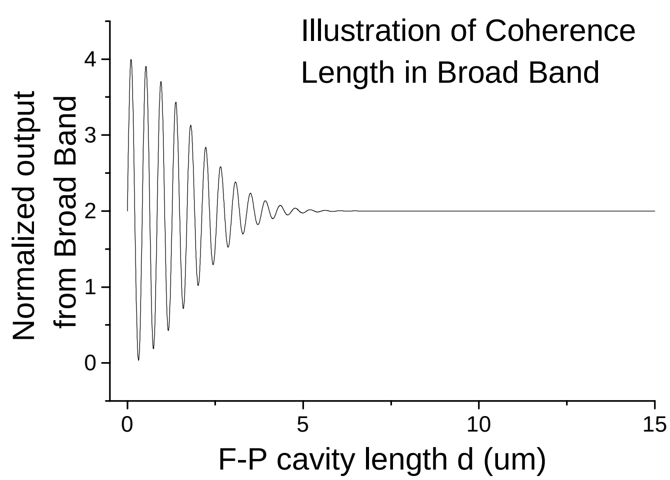

Figure 2-5. Output of Broad Band as a function of F-P cavity length d

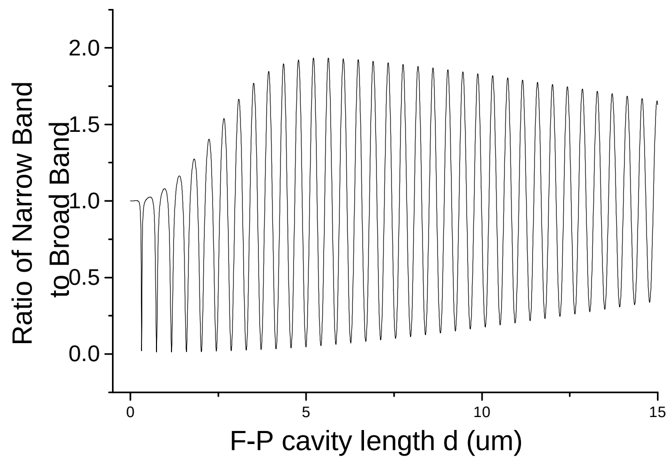

Figure 2-6. Ratio of Narrow Band to Broad Band as a function of F-P cavity length d

2.2.2 Linear Operating Range

Another key issue on design of the sensor head in the SCIIB sensor system is the choice of the linear operating range of the sensor head. When the sensor output reaches the peak or valley of an interference fringe as shown in Figure 2-7, sensitivity reduction of the sensor and the fringe direction ambiguity will occur due to the essence of the sinusoidal curve which the rule of the sensor output coheres to with the change of Fabry-Perot cavity length. At the peak or valley of a fringe, the sensitivity of the sensor will be reduced since at that point the change of output is zero for a very small change in the sensor cavity length. Fringe direction ambiguity means that it is impossible to tell the direction of sensor output change whether the Fabry-Perot cavity is increasing or decreasing from just detecting the optical intensity of the sensor output. To avoid these two problems, we design and fabricate the SCIIB sensor head to operate only over the linear range of one-half fringe, as shown in Figure 2-7, so that a one-to-one quantitative relation between the output intensity and the sensor cavity length is obtained. In our case we commonly choose the operating point between the 10% point and 90% point in one-half interference fringe for different specific applications.

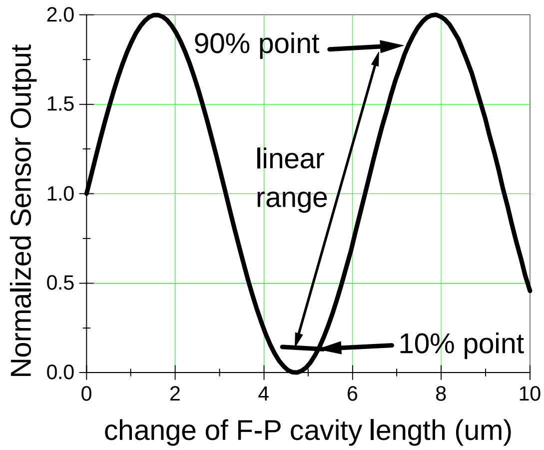

Figure 2-7. Linear Operating Range of fringes

2.2.3 Impact of Central Wavelength Drift on SCIIB Sensor System

According to the principle of the SCIIB sensor system, the validity of Split-Spectrum technique is based on the precondition that the central wavelengths of the Narrow Band and the Broad Band maintain stable during the measurement of the specified physical measurand. From the equations above for calculating outputs of the Narrow Band and the Broad Band, we can see that the outputs I_{narrow} and I_{broad} are related to the central wavelengths of the Narrow Band λ_{narrow} and the Broad Band λ_{broad}. If other factors, especially the specified physical measurand, are unchanging but λ_{narrow} and λ_{broad} are changing, the outputs I_{narrow} and I_{broad} will be changing in response to the changes of λ_{narrow} and λ_{broad}. However, because the ratio of I_{narrow} to I_{broad} are not changing linear proportionally with the changes of λ_{narrow} and λ_{broad}, thus the changes of output I_{narrow} and I_{broad} will result in undesired distortion of the ratio of I_{narrow} to I_{broad}, which will invalidate the Self-Calibration principle. Because we specify the ratio of I_{narrow} to I_{broad} as our final measurement result, thus error of measurement for specified physical measurand will occur.

Here some simulation results are shown to indicate the error due to the central wavelength drift of the Broad Band (because of the characteristic of the bandpass filter, the Narrow Band is more stable than the Broad Band). We still use the parameters defined above except $\Delta\lambda_{narrow}$=30nm for the illustration convenience.

(a)Ratio of Narrow Band to Broad Band as a function of F-P cavity length d when the central wavelength of Broad Band drifts

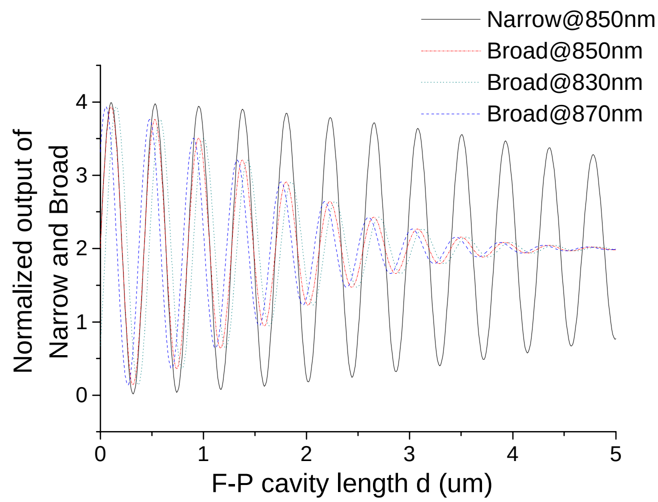

Figure 2-8. Output of Narrow Band and Broad Band as a function of F-P cavity length d with central wavelength drift of Broad Band

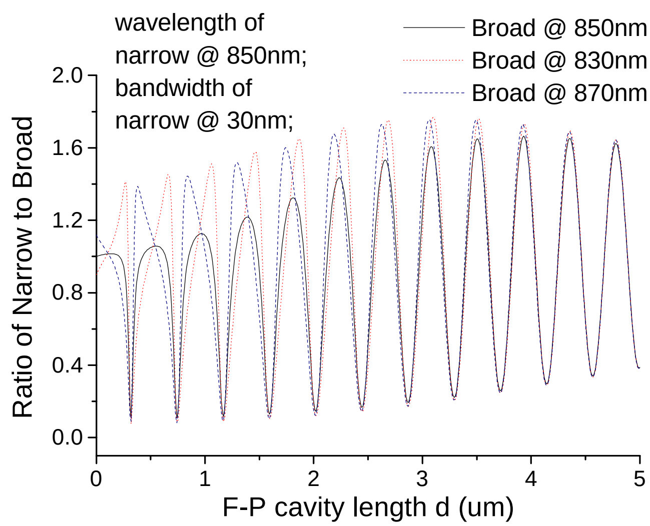

Figure 2-9. Ratio of Narrow Band to Broad Band as a function of F-P cavity length d with central wavelength drift of Broad Band

(b) Relationship between Broad Band's central wavelength drift and F-P cavity length d

In the following section we calculate the relationship between Broad Band's central wavelength drifts and the F-P cavity length d with choosing different ratios (see points in Figure 2-10).

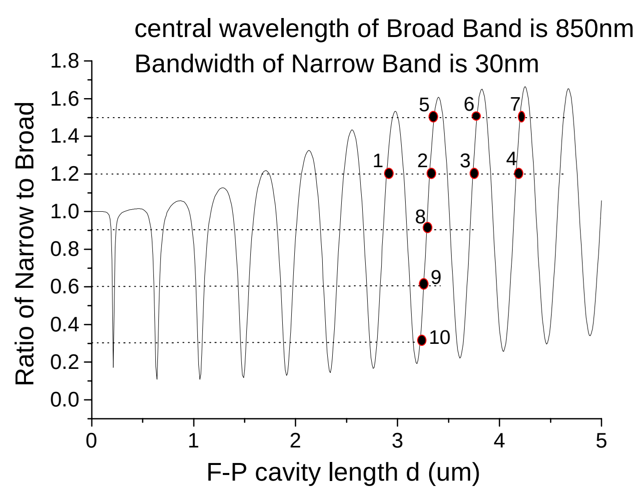

Figure 2-10. Reference model of Ratio Graph

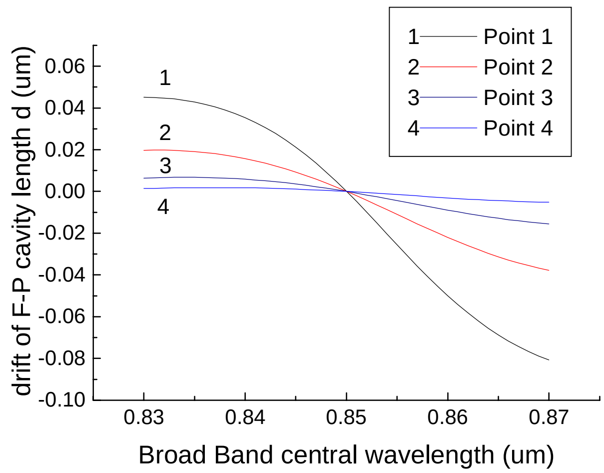

Figure 2-11. F-P cavity length d drift equivalent to Broad Band central wavelength drift (point 1,2,3,4)

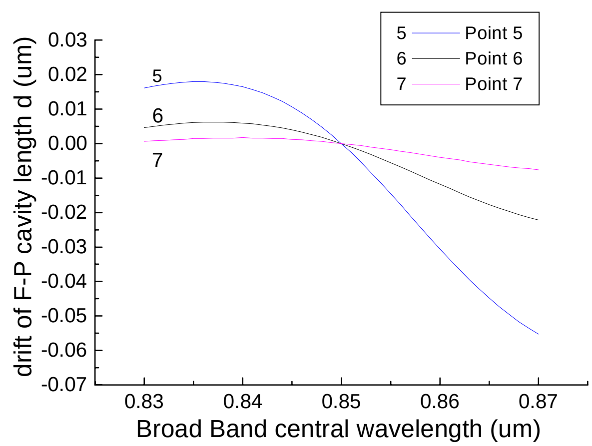

Figure 2-12. F-P cavity length d drift equivalent to Broad Band central wavelength drift (point 5,6,7)

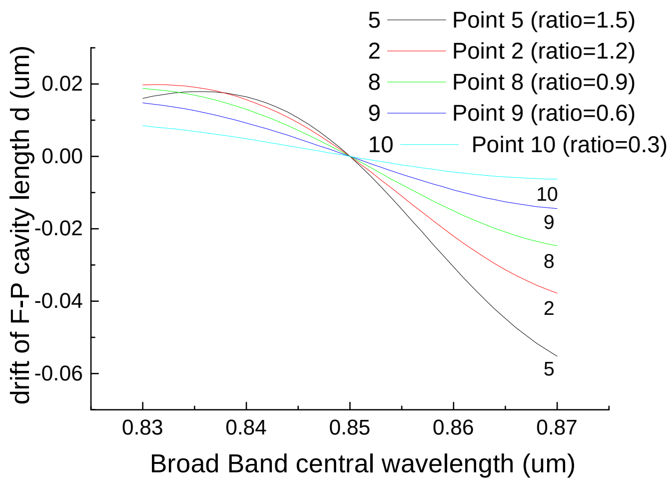

Figure 2-13. F-P cavity length d drift equivalent to
Broad Band central wavelength drift (point 5,2,8,9,10)

From Figure (2-11) and Figure (2-12), we can see that within the coherence length of Broad Band, smaller the F-P cavity length d, bigger the impact of the central wavelength drift of the Broad Band on the output result and bigger the error of the measurement. From Figure (2-13), we can see that bigger the ratio, bigger the impact of the central wavelength drift of the Broad Band on the output result and bigger the error of the measurement.

Thus according to these simulation results, we should fabricate sensor heads with F-P cavity length big enough to reduce the impact of the central wavelength drift of the Broad Band. This way will significantly improve the performance of the SCIIB sensor system with little impact of the Broad Band although there still exists the impact of the central wavelength drift of the Narrow Band.

2.3 Principle of SCIIB Temperature Fiber Optic Sensor

In essence, a Fabry-Perot fiber optic temperature sensor provides a temperature-sensitive reflectance spectrum. Due to the physical or chemical measurands' fluctuation, the physical or chemical property of the Fabry-Perot interferometer will be changed such as the structure of the F-P interferometer and the refractive index of the fiber or the tube. Here our SCIIB fiber optic temperature sensor is based on the geometric structure change caused by the corresponding environmental temperature's fluctuation. Figure 2-15 shows the geometric structure of the EFPI-based sensor head.

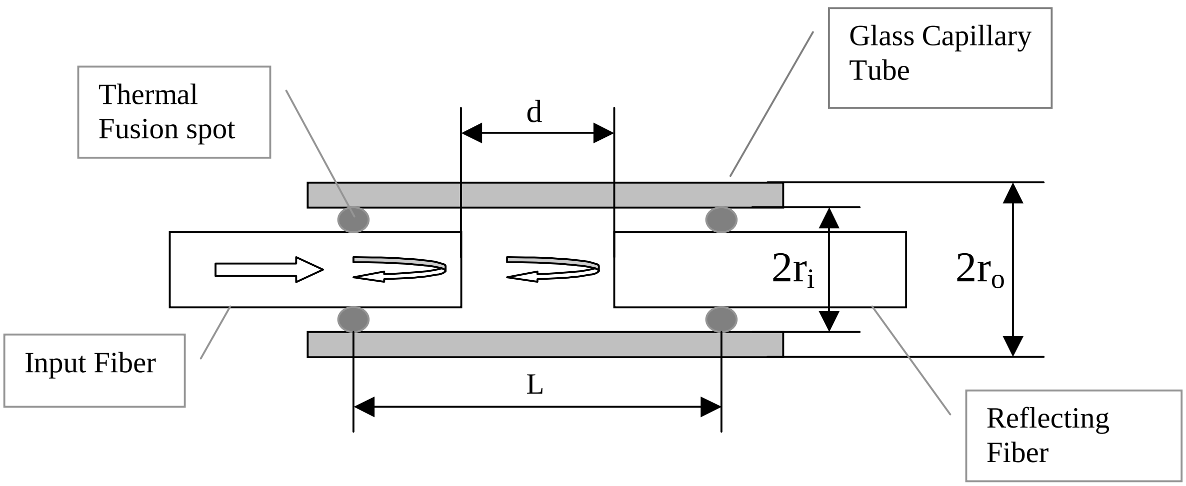

Figure 2-14 Geometry of EFPI-based Sensor Head

Based on the geometric structure of the EFPI-based sensor head, the environmental temperature variation will cause the change of the physical lengths of the capillary tube and the fibers, which results in the change of the F-P cavity length d between the two fiber end-faces. The temperature induced cavity length change will cause the sensor output drift from its original static operation point and display corresponding output reading for the temperature measurement results.

As shown in Figure 2-14, we consider the EFPI sensor head geometric structure's change in just one dimension — longitudinal direction because the thermal expansion in radial direction has no contribution to output results. We define the effective sensor gauge length (the distance between the two bonding points) as L and the air-gap length as d. If the glass capillary tube is chosen to have a coefficient of thermal expansion (CTE) of $\alpha_{h,}$

and the CTE of the fibers is α_f, then the temperature introduced F-P cavity length change Δd can be calculated by

$$\begin{aligned}\Delta d &= [L\alpha_h - (L-d)\alpha_f]\Delta T \\ &= [\alpha_f d - (\alpha_f - \alpha_h)L]\Delta T\end{aligned} \qquad (2\text{-}17)$$

where ΔT is the temperature change.

In theory, when temperature increases, the thermal expansion of the tube intends to elongate the sensor F-P cavity length. And the thermally induced expansions of the two fibers intend to shrink the cavity length. The combination of these two changes corresponds to the temperature change, resulting in output change of the sensor head. When temperature decreases, the output change of the sensor head will be in reverse direction.

2.4 Advantages of the SCIIB Sensor Technology

In addition to the generic fiber sensor advantages such as small size, lightweight, remote operation, immunity to EMI, electrically non-conducting, and chemical inertia, the unique SCIIB signal processing method combines the advantages of both interferometric and intensity-based sensors and provides the sensor a number of other major advantages as summarized as below:

1. High Resolution

Due to essence of EFPI interferometry we adopt in SCIIB sensor system, the SCIIB fiber optic sensors can provide us with a very high resolution for the measurement of various physical or chemical measurands, for example resolution for temperature measurement can reach 0.1°C.

2. Large Dynamic Range

With the optimized designed and fabricated SCIIB sensor head, SCIIB sensor system can offer us with a very large dynamic range, for example the operating range for temperature measurement can get from room temperature up to 800°C.

3. Self-Calibrated Ability

As indicated in its name, SCIIB sensor technology provides us with its excellent Self-Calibrated ability to calibrate the potential error caused by the optical power fluctuation inside the sensor system. No matter the fluctuation due to the optical source power fluctuation or the transmitting fiber loss, SCIIB sensor system can compensate the fluctuation automatically.

4. Simple Signal Processing Technique

As described before, SCIIB sensor technology employs intensity-based fiber optic sensors' signal processing technique — directly detecting the optical intensity with photodetectors. Thus on one hand it can provide us with high resolution and precision, on the other hand it can maintain our signal processing mechanism as simply as possible.

5. Absolute measurement

According to the principle of SCIIB sensor technology, we utilize the linear range in one half of an interference fringe as the operating range of the SCIIB sensor. Hence the sensor output is a unique, almost linear function of the change of the F-P cavity length. This one-to-one quantitatively relationship between the sensor output and the F-P cavity length makes it possible to measure the absolute value of the sensor F-P cavity length after we select and fix the initial cavity length.

6. Design and Fabrication Flexibility

The SCIIB sensor head employs Extrinsic Fabry-Perot Interferometer structure which is simple and easy for us to design and fabricate. It offers us a great design and fabrication flexibility to accommodate the requirements for different applications.

7. Suitability for Harsh Environment

The SCIIB sensors are suitable for monitoring and control of physical or chemical measurands such as aircraft engines, conventional and nuclear power plants, industrial plants, and other systems in which conditions could be too severe for electronic temperature sensors (thermocouples, thermistors, and bimetallic devices). Unlike electronic temperature sensors, these and other photonic temperature sensors do not pose a sparking hazard and are insensitive to electromagnetic interference at suboptical frequencies.